

RSC Advances



This is an *Accepted Manuscript*, which has been through the Royal Society of Chemistry peer review process and has been accepted for publication.

Accepted Manuscripts are published online shortly after acceptance, before technical editing, formatting and proof reading. Using this free service, authors can make their results available to the community, in citable form, before we publish the edited article. This *Accepted Manuscript* will be replaced by the edited, formatted and paginated article as soon as this is available.

You can find more information about *Accepted Manuscripts* in the [Information for Authors](#).

Please note that technical editing may introduce minor changes to the text and/or graphics, which may alter content. The journal's standard [Terms & Conditions](#) and the [Ethical guidelines](#) still apply. In no event shall the Royal Society of Chemistry be held responsible for any errors or omissions in this *Accepted Manuscript* or any consequences arising from the use of any information it contains.

TiO₂-Graphene Hybrid Nanostructures by Atomic Layer Deposition with Enhanced Electrochemical Performance for Pb(II) and Cd(II) Detection

Hongfen Zhang^{a,c}, Shaomin Shuang^c, Guizhen Wang^b, Yujing Guo^c, Xili Tong^b, PengYang^b, Anjia Chen^a,
Chuan Dong^{c*} and Yong Qin^{b*}

Received (in XXX, XXX) Xth XXXXXXXXX 20XX, Accepted Xth XXXXXXXXX 20XX

DOI: 10.1039/b000000x

ABSTRACT In this work, atomic layer deposition is applied to coat graphene nanosheets with TiO₂. The produced TiO₂-Graphene (TiO₂-Gr) composites are characterized by X-ray photoelectron spectroscopy, fourier transform infrared spectroscopy, and transmission electron microscopy. It is revealed that TiO₂ are effectively deposited on the surface of graphene. The coatings have a highly controlled thickness. The electrochemical properties of the obtained TiO₂-Gr composites are investigated for detection of lead (Pb²⁺) and cadmium (Cd²⁺) ions by differential pulse anodic stripping voltammetry (DPASV). It is found that the TiO₂-Gr composite exhibits improved sensitivity for detection of these metal ions. The linear dynamic ranges are from 1.0×10⁻⁸ M to 3.2×10⁻⁵ M for Pb²⁺ and 6.0×10⁻⁷ M to 3.2×10⁻⁵ M for Cd²⁺, respectively. The detection limits (S/N = 3) are estimated to be 1.0×10⁻¹⁰ M for Pb²⁺ and 2.0×10⁻⁹ M for Cd²⁺, respectively.

1. Introduction

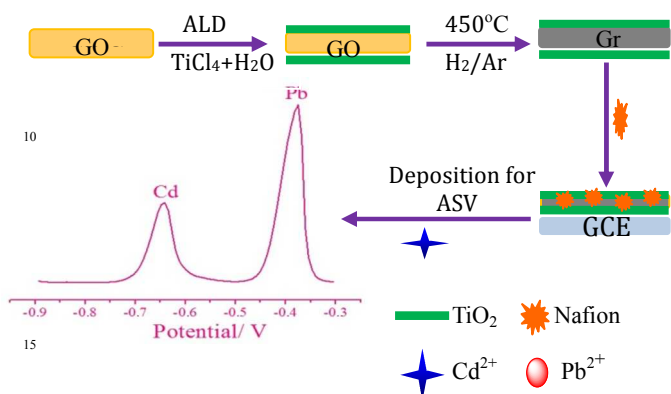
In recent years, a wide variety of nanomaterials, in particular nanoparticles with different functions, have been found broad applications in analytical detection fields.¹ Owing to their small size, nanoparticles exhibit unique chemical, physical and electronic properties that are different from those of bulk materials, and can be used to construct novel sensing devices, in particular, electrochemical sensors and biosensors.^{2,3} Titanium dioxide is considered to be an attractive compound because of their low cost, excellent chemical stability, nontoxicity to the atmosphere and high surface area.⁴⁻¹² As a “rising star” material, graphene has attracted considerable attention from both experimental and theoretical scientific communities owing to its unique two-dimensional structure and a variety of fascinating thermal, mechanical, and electrical properties.¹³ New properties can result from the coating of graphene by different materials.¹⁴⁻¹⁸ However, traditional methods were subject to intrinsic limitations in the precise control of thickness and coating quality. Simple and effective approaches for the controllable synthesis of graphene hybrid nanostructures are desired for an optimized performance of the composite. Atomic layer deposition (ALD) is a high-level film technology which allows growth of dense thin films with atomic-level precision in a layer-by-layer manner. Its outstanding advantages make ALD a high efficient approach for the controllable synthesis of TiO₂-graphene (TiO₂-Gr) hybrid nanostructures.^{19,20}

As is well known, lead and cadmium pose severe risks to human health with toxic effects on living organism. For example, the toxicity of lead in humans mainly comes from its detrimental mimicking action by occupying the

calcium binding sites on numerous calcium-dependent proteins in cells (such as, calmodulin and enzyme protein kinase C), thus resulting in the corresponding impairment of physiological functions.^{21,22} Therefore, a sensitive, rapid and simple analytical method for precise monitoring of Pb²⁺ and Cd²⁺ has been always a matter of utmost need. However, development of inexpensive, rapid, and reliable portable sensors for individual and especially simultaneous quantification of trace/ultra-trace levels of Pb and Cd is still a challenge. Such sensors should also have high specificity for Pb and Cd, high measurement frequency and precision and infrequent regeneration of sensor material. Electrochemical sensors appear to meet all these needs.²³ Differential pulse anodic stripping voltammetry (DPASV) has proved to have remarkable sensitivity and suitability for determination of trace and ultra-trace levels of Pb and Cd. Mercury based electrodes have been most widely used in DPASV of Pb and Cd^{24,25} due to their wide potential window toward negative potential values. However, the recent trends toward green chemistry aim to reduce and eliminate use of mercury. It is known that the electrode performances depend on both the catalyst and supporting material.

Much attention was recently paid to the synthesis and application of TiO₂-Gr composites mainly used for supercapacitor and photocatalysis.²⁶⁻²⁹ Here we report the synthesis of TiO₂-Gr hybrid nanostructures by ALD. The products have been characterized by X-ray photoelectron spectroscopy (XPS), Fourier transform infrared spectroscopy (FTIR), transmission electron microscopy (TEM), and cyclic voltammetry. Their electroanalytical capability for sensing of Pb(II) and Cd(II) ions was investigated. The composites exhibited excellent performance for the analysis of Pb²⁺ and Cd²⁺ by combining the advantages of the graphene nanosheets

(high electrical conductivity and specific area) with the unique features of the TiO₂ coating. To our knowledge, TiO₂-Gr composites by ALD have not been investigated up to date as electrode materials for electroanalytical determination of heavy metals.



Scheme 1 Illustration of the procedure for preparing TiO₂-Gr nanocomposites and the electrochemical sensing strategy for Pb²⁺ and Cd²⁺ detection.

2. Experimental

2.1. Reagents

Graphite was purchased from Alfa Aesar. Hydrazine solution (50 wt%) and ammonia solution (25–28 wt%) were obtained from Beijing Chemical Reagent Company (Beijing, China). Titanium tetrachloride (TiCl₄, 99.8%) was purchased from Strem Chemicals. Nafion (5 wt% in low aliphatic alcohols) was purchased from Aldrich (Milwaukee, WI) and then diluted to 1 wt% Nafion with 2-propanol. Stock solutions of Pb²⁺ and Cd²⁺ were prepared by diluting the corresponding standard stock solutions prepared with CdCl₂ and PbCl₂, respectively. A 0.1 M acetate buffer (pH 4.5) prepared by mixing appropriate amounts of CH₃COOH and CH₃COONa, was used to prepare solution of the supporting electrolyte. Unless otherwise stated, all solutions were prepared with deionized water. All chemicals employed in this experiment were of chromatographic reagent grade.

2.2. Apparatus

DPASV was performed in a conventional three-electrode cell with a CHI 842B electrochemical workstation (CH Instruments, Shanghai, China). A glassy carbon (3mm in diameter) electrode (GCE) modified with Nafion-TiO₂-Gr was served as the working electrode. An Ag/AgCl (saturated KCl) electrode and a platinum foil were used as the reference electrode and auxiliary electrode, respectively. TEM images were taken on a JEOL-2100F microscope. The composition of the samples was analyzed by energy dispersive x-ray spectrometry (EDX) attached to the TEM instrument. The ALD process was carried out in a hot-wall closed

chamber-type ALD reactor. Fourier transform infrared spectra were recorded on a Bruker Tensor 27 spectrometer (Germany). XPS measurements were carried out using a Kratos XSAM800 with Al K-X-ray radiation as the X-ray source for excitation.

2.3. Synthesis of TiO₂-Gr nanocomposites

Graphene oxide (GO) was synthesized from natural graphite by Hummers' method.³⁰ Briefly, graphite powders (5g, 20 μm) were added to a mixture of concentrated H₂SO₄ (115 mL) and NaNO₃ (2.5 g). The solution was stirred in an ice bath (0 °C), added carefully with KMnO₄ (15 g) and then maintained for 30 min at 35 °C. Further, deionized water (230 mL) was slowly added to the solution. The temperature of the solution was then raised to 98 °C for 15 min. Afterwards, additional deionized water (355 mL) containing H₂O₂ (3 wt%, 5 mL) was added to the solution. A solid was obtained by centrifugation (13000 rpm, 20 min) followed by rinsing with excess deionized water, 20 vol% HCl and ethanol. The rinsing process was repeated three times. The final yellow brown GO powders were then dried in vacuum at 40 °C for 12 h.

Prior to ALD, the graphene oxide (GO) was dispersed in ethanol by ultrasonic agitation and then dropped onto a quartz wafer. After being air-dried, a TiO₂ layer was first deposited by ALD at 150 °C using TiCl₄ and water as the titanium and oxygen source, respectively. After the ALD process, the samples were transferred to a furnace and reduced at 450 °C in 5% H₂/Ar atmosphere for 2 h. Finally, powder of TiO₂-Gr composite was obtained.

2.4. Fabrication of the Nafion-TiO₂-Gr composite film

Ultrasonic agitation was used to disperse the TiO₂-Gr nanocomposites into 100 μL 1 wt% Nafion-isopropyl-alcohol to give 0.25 mg·mL⁻¹ Nafion-TiO₂-Gr suspension. Prior to modification, the GCE was polished with 1, 0.3 and 0.05 μm alumina slurry, rinsed thoroughly with doubly distilled water between each polishing step, then washed successively with 1:1 nitric acid, acetone and doubly distilled water in ultrasonic bath and dried in air. The Nafions/GCE and Nafion-TiO₂-Gr/GCE were obtained by casting 5 μL of 0.25 mg/mL Nafions or Nafion-TiO₂-Gr suspension on the surface of well-polished GCE and dried under an infrared lamp.

2.5. Procedure for DPASV analysis

The three electrodes were immersed into the electrochemical cell, containing 5 mL 0.1 M acetate buffer (pH 4.5) and the target metal ions. The GCE modified with Nafion-TiO₂-Gr was placed in situ with the target metals by spiking the test solution with different concentrations of Pb²⁺ and Cd²⁺ and depositing the target metals on the surface of the electrode at -1.2 V under stirring for 120 s. Following the preconcentration step, the stirring was stopped and after 10 s the voltammogram was recorded by applying a positive-going differential pulse voltammetry scan (with a

step increment of 7mV, amplitude of 80 mV, and pulse period of 1 s). The scan was terminated at 0 V. Prior to the next cycle, a preconditioning step (60 s at 0.3 V, with solution stirring) was used to remove the target metals. Scheme 1 shows the procedure for preparing TiO₂-Gr and the sensing step of target metal ions by electrochemical strategy..

3. Results and discussion

3.1. Characterization of TiO₂-Gr

It is well known that ALD of TiO₂ on pristine graphene has initial nucleation difficulties because the graphene basal plane is very inert. TiO₂ nanoparticles were produced when TiO₂ nucleates and grows only at defect sites on the graphene surface.³¹ There are some researches on the synthesis of TiO₂-Gr nanocomposites by ALD with the assistance of a thin layer of Al₂O₃ as an adhesion layer.³²⁻³³ In this work, to overcome this shortcoming, TiO₂ ALD was directly deposited on the reactive graphene oxide nanosheets, which contain a great number of carboxyl, epoxide, and phenolic hydroxyl functional groups. Then the graphene oxide covered by TiO₂ was reduced at 450 °C in 5% H₂/Ar atmosphere. Thus, a facile and fast method was successfully developed to fabricate TiO₂-Gr hybrid nanostructures by ALD method in our study.

TEM was used to characterize the thickness and morphology of the TiO₂-Gr. Fig. 1A displays a representative TEM image of GOs, indicating a single-layer structure. As observed from the TEM image shown in Fig. 1 B, a TiO₂ film with a thickness of about 4 nm is coated on the GOs by applying 100 ALD cycles for TiO₂ deposition. the advantages of ALD enable us to easily control the thickness of TiO₂ layers by changing the cycle number. Fig. 1C-F shows the TEM images of TiO₂-Gr obtained by applying 20, 50, 70 and 100 ALD cycles for TiO₂ deposition, respectively. It can be found that the thickness of TiO₂ layers clearly increases with the increase of ALD cycles. It amounts to about 1.0, 2.0, 3.5, and 5.0 nm, respectively, which corresponds to a growth rate of about 0.5 Å per cycle. High resolution TEM (HRTEM) investigations were conducted in order to investigate the crystalline structure of the TiO₂ coatings. It can be seen that the TiO₂ coatings have an interplanar spacing of 3.5 Å (Fig. 1G,H), matching well with the (101) plane of a crystalline anatase structure.

The formation of TiO₂-Gr composite was verified by FTIR spectra (Fig. 2). In the spectrum of GO, the band at 3600 cm⁻¹ indicates the presence of free or associated hydroxyl groups (-OH), resulted from adsorbed bound water or -OH linked to the basal plane of GO. There are also bands owing to carboxyl C=O (1733 cm⁻¹) and C=C (1580cm⁻¹) groups, and alkoxy C-O (1059 cm⁻¹) groups located at the edges of the GO nanosheets.³⁴As for graphene (red line), the intensity of the absorption bands of the C=O (1725 cm⁻¹) and C-O (1061 cm⁻¹) groups decrease significantly or even disappear, indicative of the formation of graphene after GO sample was reduced at 450 °C in 5%

H₂/Ar atmosphere. The absorption band centered at 3600 cm⁻¹ is attributed to the residual -OH groups of GO. The C=O stretching band disappears in the FTIR spectrum of TiO₂-Gr, revealing that the C=O groups are almost removed in the process of reduction. The FTIR spectra of the TiO₂-Gr show a broad band below 1000 cm⁻¹, which can be attributed to a combination of Ti-O-Ti vibration and Ti-O-C vibration (798 cm⁻¹).^{35,36} Meanwhile, the intensity of the absorption band of C-O groups (1052 cm⁻¹) increases significantly. These data demonstrate that TiO₂-Gr hybrid nanostructures have been successfully synthesized by ALD.

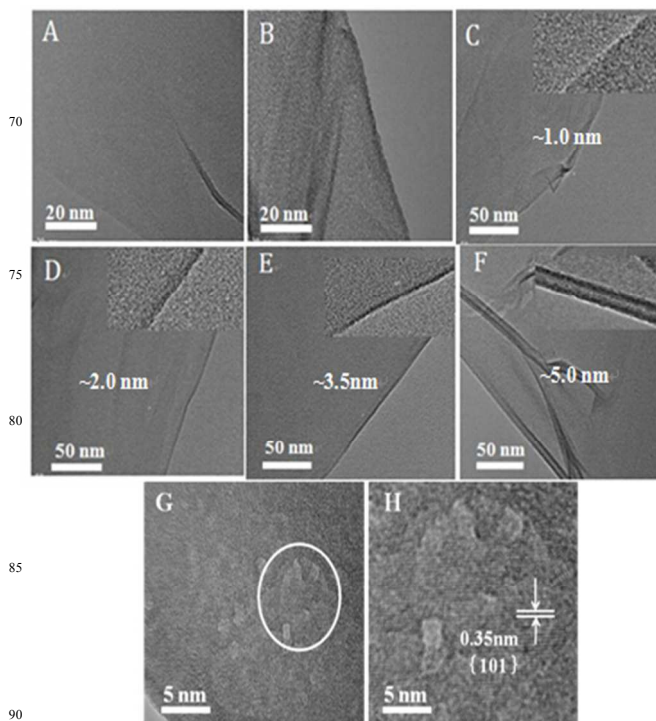


Fig. 1 TEM image of (A) the pristine GOs, (B) GOs coated with TiO₂ by applying 100 ALD cycles, (C), (D), (E) and (F) TiO₂-Gr obtained by applying 20, 50, 70 and 100 ALD cycles for TiO₂ deposition, respectively (inset: corresponding amplified images of the TiO₂-Gr). (G) HRTEM image of the TiO₂-Gr after 100 ALD cycles for TiO₂ deposition. (H) Amplified image of the area marked with a circle in panel G.

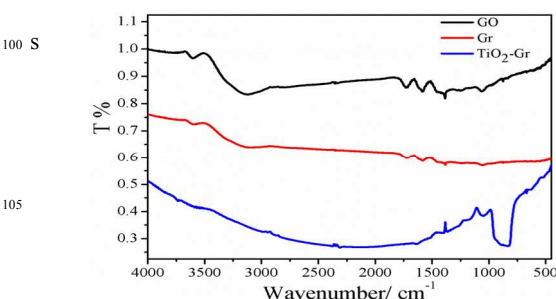


Fig. 2 FTIR spectra of GO (black line), Gr (red line) and TiO₂-Gr (blue line)

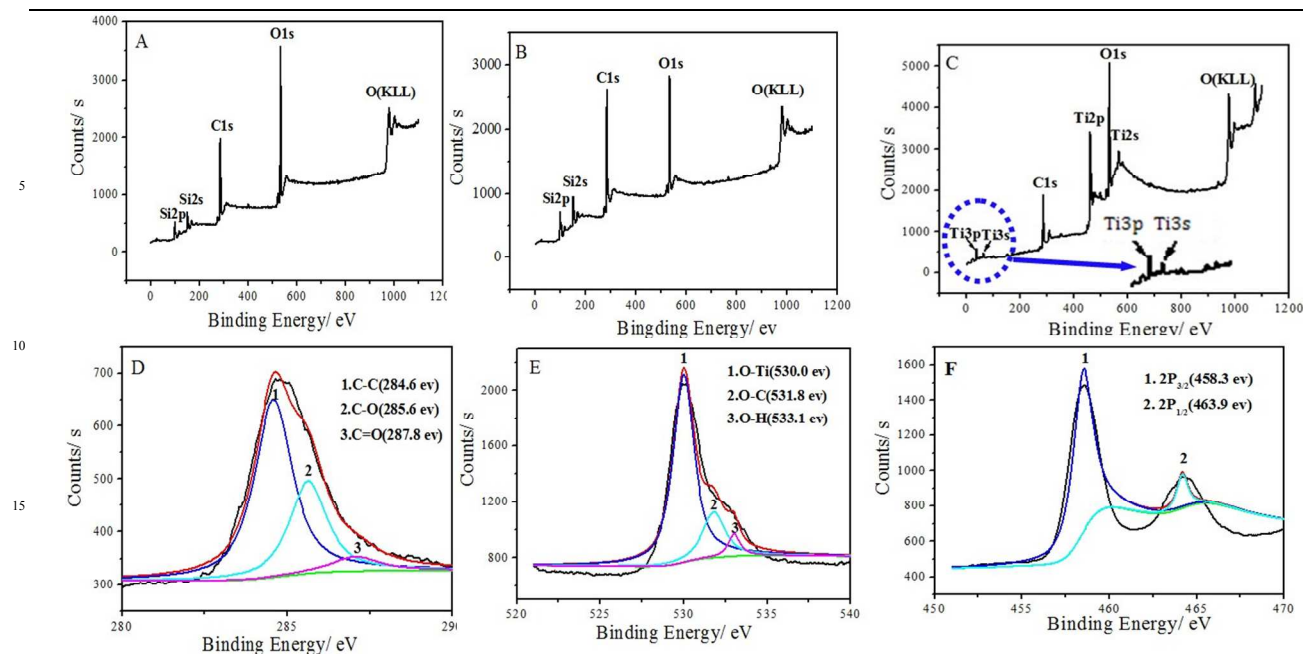


Fig. 3 The survey XPS data for GO (A), Gr (B) and TiO₂-Gr (C); The deconvolution of C1s (D), O1s (E) and Ti2p (F) spectra of TiO₂-Gr composite grown by applying 100 TiO₂ ALD cycles,

XPS was also used to characterize the GO, Gr, and TiO₂-Gr composite. The surveys (Fig. 3A, B) of GO and Gr reveal the absence of Ti2s at about 568 eV, Ti3p at about 37 eV and Ti3s at about 61 eV, respectively. Compared with GO and Gr, the survey of TiO₂-Gr (Fig. 3C) shows the presence of Ti2s, Ti2p, Ti3s and Ti3p originating from TiO₂, further indicating the successful coating of TiO₂ on graphene by ALD. Fig. 3D shows the corresponding high resolution XPS and curve fitting of the C1s peaks. The energies at 284.6, 285.6, and 287.8 eV can be assigned to C-C, C-O, and C=O, respectively.³⁷ However, we did not observe any peak corresponding to Ti-C bond at ~282 eV (C1s), suggesting no carbon doping in the lattice of TiO₂.³⁸ The O1s spectra displayed in Fig. 3E can be fitted with three peaks. The main peak at 530.0 eV is assigned to the Ti-O bond, while the peaks at 531.8 and 533.1 eV are raised from the C-O bond and the H-O bond, respectively.³⁹ It can be seen from Fig. 3F that the binding energies for Ti 2P_{1/2} and Ti 2P_{3/2} are located at 463.9 and 458.3 eV with a peak separation of 5.6 eV, implying the presence of the normal state of Ti⁴⁺ in the TiO₂-Gr composites. These results are also consistent with the chemical linkage between TiO₂ and graphene.³⁹⁻⁴² This chemical bonding may facilitate the fast electron transport throughout the graphene network and between the graphene and the anchored TiO₂ nanostructure.

3.2. Electrochemical characterization of the TiO₂-Gr composite

Electrochemical experiments were used to characterize the TiO₂-Gr composite. Different cyclic voltammograms (CVs) at bare, Nafion-Gr, and Nafion-TiO₂-Gr modified GCE in a freshly prepared solution containing 2 mM K₃Fe(CN)₆ in the presence of 0.1 M KCl are shown in Fig. 4(A). A well-shaped CV with a peak-to-peak separation of 66 mV is observed at the bare GCE (line 1). After being modified with Nafion-Gr (line 2) and Nafion-TiO₂-Gr (line 3), the intensity of all anodic and cathodic peaks decrease. The phenomena are different with our previous result^{16,43} which should be ascribed only to Nafion, demonstrating that the negative charged skeleton of Nafion acted as the blocking layer for the diffusion of Fe(CN)₆³⁻ into the film and hindered the electron and mass transfer.⁴⁴ However, at the Nafion-TiO₂-Gr modified GCE, the peak current increases obviously unlike that observed at Nafion-Gr modified GCE, indicating that the introduction of the TiO₂-Gr provides better conducting bridges for the electron transfer of Fe(CN)₆³⁻.

Fig. 4B shows the DPASV analytical characteristics of GCEs coated with different films, e.g., Nafion-TiO₂-Gr (line a) and Nafion-Gr (line b) for Pb²⁺ and Cd²⁺ determination. The stripping voltammograms were obtained in a solution containing 1.0 × 10⁻⁵ M each of Pb²⁺, Cd²⁺ in 0.1 M acetate buffer (pH 4.5) without deaeration. The sharper and higher peak current for the target metal ions were obtained at the Nafion-TiO₂-Gr modified electrode. Compared with the Nafion-Gr-coated electrode, the analytical signals are improved about 1.2-fold and 12.5-fold, respectively. This can be attributed to the following factors: (i) the change of the morphologies and the structure of interface, and (ii) modification of the

interfacial electron-transfer (iii) the enhanced adsorption capacity of TiO₂ coatings for heavy metal ions.^[45] In order to verify these possibilities, ESI, a powerful technique, was used to obtain the information on the impedance changes of the electrode surface. Compared with that of the Nafion-Gr modified electrode, the electron-transfer resistances of the Nafion-TiO₂-Gr sensing platform reduce greatly (Fig. 4(B) Insets). This is resulted from the high conductivity due to the extensive conjugated sp² carbon network⁴⁶ and TiO₂ assisted ion transport.^[4,12]

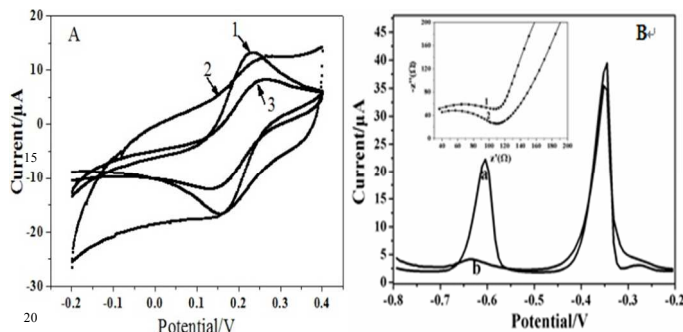


Fig. 4 (A) CVs for bare (line 1), Nafion-Gr modified (line 2) and Nafion-TiO₂-Gr modified (line 3) GCE in 2 mM K₃Fe(CN)₆ containing 0.1 M KCl, at a scanning rate of 50 mVs⁻¹. (B) DPASV's for 1.0 × 10⁻⁵ M each of Cd²⁺ and Pb²⁺ on Nafion-TiO₂-Gr modified GCE (line a) and Nafion-Gr modified GCE (line b), respectively. The inset shows the EIS characterization of the sensing interfaces: (1) Nafion-Gr modified GCE, (2) Nafion-TiO₂-Gr modified GCE.

3.3 The effect of the experimental variables

The effect of the deposition potential on the peak current of Cd²⁺ and Pb²⁺ after 120 s accumulation was studied in the potential range from -1.3 V to -0.9 V. The obtained results are shown in Fig. 5(A). When the accumulation potential shifts from -0.9 V to -1.2 V, the stripping peak currents increase. As the accumulation potential becomes more negative than -1.2 V, the peak current reduces obviously. To obtain a good sensitivity for both Cd²⁺ and Pb²⁺ detection, -1.2V was used as the optimal accumulation potential for the subsequent experiment.

The accumulation time is another important factor that influences the sensitivity of the proposed method. As depicted in Fig. 5(B), with the increase of the deposition time, the response of the stripping peak currents of 5.0 × 10⁻⁶ M Cd²⁺ and Pb²⁺ increases with the preconcentration time due to the increased amount of analytes on the Nafion-TiO₂-Gr modified electrode. However, the peak current decreases after 120 s because of the rapid surface saturation, which lowers the upper detection limit. Therefore, 120 s was chosen as the optimal accumulation time.

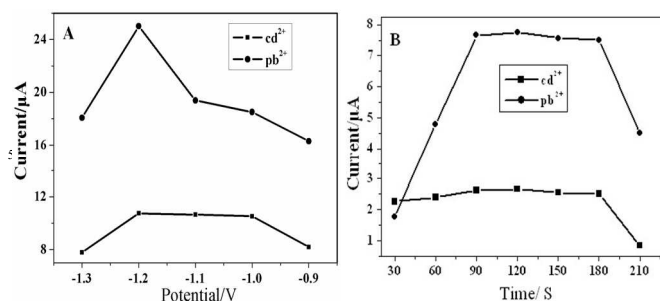


Fig. 5 Effect of the accumulation potential (A) and deposition time (B) on the stripping peak current of 5.0 × 10⁻⁶ M each of Cd²⁺ and Pb²⁺ on a Nafion-TiO₂-Gr modified electrode.

3.4 Sensing of Pb²⁺ and Cd²⁺ at Nafion-TiO₂-Gr/GCE

Calibration plots for the simultaneous determination of Cd²⁺ and Pb²⁺ on the Nafion-TiO₂-Gr/GCE were achieved in 0.1 M acetate buffer by increasing Cd²⁺ and Pb²⁺ concentrations from 1.0 × 10⁻¹⁰ M to 3.2 × 10⁻⁵ M. The DPASV responses for different concentrations of Cd²⁺ and Pb²⁺ are illustrated in Fig. 6. The resulting calibration plots are linear over the range from 6.0 × 10⁻⁷ M to 3.2 × 10⁻⁵ M and 1.0 × 10⁻⁸ M to 3.2 × 10⁻⁵ M for Cd²⁺ and Pb²⁺ under the optimum conditions, respectively. The calibration curves and correlation coefficients are $y = 0.3933x - 1.147$, $R^2 = 0.9904$ for Pb²⁺, $y = 1.9375x - 2.184$, $R^2 = 0.9878$ for Cd²⁺, respectively (x : concentration/mol · L⁻¹, y : current/μA). Based on three times the background noise, the limits of detection were 2.0 × 10⁻⁹ M for Cd²⁺ and 1.0 × 10⁻¹⁰ M for Pb²⁺, respectively, revealing a wider or comparable linear response to Pb²⁺ and Cd²⁺. Compared with most of the previous electrochemical methods for Pb²⁺ and Cd²⁺ detection⁴⁷⁻⁵⁰, the present method shows a comparable sensitivity. The specific features of this method are shown in Table 1.

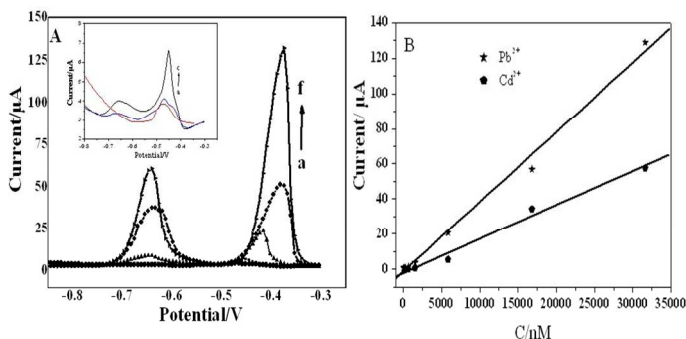


Fig. 6 (A) the DPASV signals of Cd²⁺ and Pb²⁺ with different concentrations. (B) the linear relationship between the concentration of metals and peak current

Table 1 Comparison of analytical merits achieved using electrochemical methods for the determination of Pb²⁺ and Cd²⁺.

Metal ions	Linear range (M)	Detection limit (M)	Reference
Pb ²⁺ Cd ²⁺	2.4 × 10 ⁻⁹ ~4.3 × 10 ⁻⁷ 4.4 × 10 ⁻⁹ ~8.1 × 10 ⁻⁷	7.2 × 10 ⁻¹⁰ 8.9 × 10 ⁻⁹	[47]
Pb ²⁺ Cd ²⁺	1.0 × 10 ⁻⁵ ~1.0 × 10 ⁻⁴ 1.0 × 10 ⁻⁵ ~1.0 × 10 ⁻⁴	2.7 × 10 ⁻⁸ 5.2 × 10 ⁻⁸	[48]
Pb ²⁺ Cd ²⁺	1.0 × 10 ⁻⁷ ~1.5 × 10 ⁻⁵ 2.5 × 10 ⁻⁷ ~2.5 × 10 ⁻⁵	1.0 × 10 ⁻⁸ 4.0 × 10 ⁻⁸	[49]
Pb ²⁺ Cd ²⁺	4.8 × 10 ⁻¹⁰ ~1.4 × 10 ⁻⁷ 8.9 × 10 ⁻¹⁰ ~1.8 × 10 ⁻⁷	2.4 × 10 ⁻¹⁰ 8.9 × 10 ⁻⁹	[50]
Pb ²⁺ Cd ²⁺	1.0 × 10 ⁻⁸ ~3.1 × 10 ⁻⁵ 6.0 × 10 ⁻⁷ ~3.2 × 10 ⁻⁵	1.0 × 10 ⁻¹⁰ 2.0 × 10 ⁻⁹	Present work

3.5 Tolerance of composites for foreign substances

Under the optimum conditions, the effect of several possible interfering substances, such as Ag⁺, Hg²⁺, Cr³⁺, Co²⁺, Zn²⁺, Ca²⁺ and Fe³⁺ on the Pb²⁺ and Cd²⁺ sensor based on the Nafion-TiO₂-Gr/GCE was investigated when the concentration of Pb²⁺ and Cd²⁺ were 1.0 × 10⁻⁵ M. Table 2 shows the results by adding 2.0 × 10⁻⁴ M of the above metals. It can be found that Ag⁺, Cr³⁺, Zn²⁺, Ca²⁺, Fe³⁺, Hg²⁺ and Co²⁺ have no effect on the assay.

Table 2. Effect of the foreign substances on the system.

Substances (%)	Determination ions	Change of ΔI_p
Ag ⁺	Pb ²⁺	+4.75
	Cd ²⁺	-5.52
Cr ³⁺	Pb ²⁺	-3.58
	Cd ²⁺	+5.29
Ca ²⁺	Pb ²⁺	-6.78
	Cd ²⁺	-4.89
Zn ²⁺	Pb ²⁺	-5.89
	Cd ²⁺	+5.44
Fe ³⁺	Pb ²⁺	-7.98
	Cd ²⁺	-5.42
Co ²⁺	Pb ²⁺	-9.68
	Cd ²⁺	+6.64
Hg ²⁺	Pb ²⁺	+0.89
	Cd ²⁺	+8.99

Conclusions

In summary, a facile and fast method was successfully developed to fabricate TiO₂-Gr hybrid nanostructures by ALD method with conveniently and highly controlled thickness for TiO₂. Ultrasensitive electrochemical detection of Pb(II) and Cd(II) based on the composite was established. Nafion-TiO₂-Gr exhibited good electrocatalytic activity towards the oxidation of Pb and Cd. The peak currents possess a linear relationship with the concentration of Pb²⁺ in the range of 1.0 × 10⁻⁸ ~ 3.2 × 10⁻⁵ M with a detection limit of 1.0 × 10⁻¹⁰ M, and of Cd²⁺ in the

range of 6.0 × 10⁻⁷ ~ 3.2 × 10⁻⁵ M with a detection limit of 2.0 × 10⁻⁹ M, respectively. To the best of our knowledge, this is the first report that electrode materials prepared by graphene with TiO₂ by ALD was applied for electroanalytical determination of heavy metals. ALD can open up new avenues to synthesize other multifunctional graphene materials with excellent photochemical or electrochemical properties.

Acknowledgments

This research work was supported by the National Natural Science Foundation of China (Nos. 21175086, 81241137 and 21275093) by the Science and Technology Innovation Fund of Shanxi Medical University (Nos. 01201305), Research Project Supported by Shanxi Scholarship Council of China (2013-152), the Hundred Talent Program of the Chinese Academy of Sciences, and the Hundred Talent Program of Shanxi Province.

Notes and references

^a School of Pharmaceutical Science, Shanxi Medical University, Taiyuan 030001, China. Tel: (+86)-351-4690071;

^b State Key Laboratory of Coal Conversion, Institute of Coal Chemistry, Chinese Academy of Sciences, Taiyuan 030001, China. Fax: (+86)-351-4040081; Tel: (+86)-351-4040081; E-mail: qinyong@sxicc.ac.cn;

^c Institute of Environmental Science, and School of Chemistry and Chemical Engineering, Shanxi University, Taiyuan, 030006, China. Fax: (+86)-351-7011011; Tel: (+86)-351-7011011 E-mail: dc@sxu.edu.cn;

- S. G. Penn, L. He and M. J. Natan, *Curr. Opin. Chem. Biol.*, 2003, **7**, 609.
- S. J. Guo and S. J. Dong, *Chem. Soc. Rev.*, 2011, **40**, 2644.
- A.Z. Shabi and H. S. Jae, *Int. J. Electrochem. Sci.*, 2014, **9**, 4598.
- G. Armstrong, A. R. Armstrong, P. G. Bruce, P. Reale and B. Scrosati, *Adv. Mater.*, 2006, **18**, 2597.
- A. R. Armstrong, G. Armstrong, J. Canales and P. G. Bruce, *Angew. Chem., Int. Ed.*, 2004, **43**, 2286.
- M. Zukalova, M. Kalbac, L. Kavan, I. Exnar and M. Gratzel, *Chem. Mater.*, 2005, **17**, 1248.
- Y. K. Zhou, L. Cao, F. B. Zhang, B. L. He and H. L. Li, *J. Electrochem. Soc.*, 2003, **150**, A1246.
- Y. S. Hu, L. Kienle, Y. G. Guo and J. Maier, *Adv. Mater.*, 2006, **18**, 1421.
- E. Baudrin, S. Cassaignon, M. Koesch, J. P. Jolivet, L. Dupont and J. M. Tarascon, *Electrochem. Commun.*, 2007, **9**, 337.
- C. H. Jiang, I. Honma, T. Kudo and H. S. Zhou, *Electrochem. Solid-State Lett.*, 2007, **10**, A127.

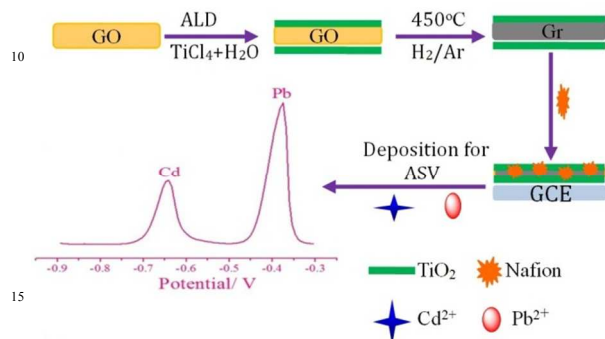
- 11 M. A. Reddy, M. S. Kishore, V. Pralong, V. Caignaert U. V. Varadaraju and B. Raveau, *Electrochem. Commun.*, 2006, **8**, 1299.
- 12 J. Moskon, R. Dominko, M. Gaberscek, R. Cerc-Korosec and J. Jamnik, *J. Electrochem. Soc.*, 2006, **153**, A1805.
- 5 13 K. S. Novoselov, V. I. Fal'ko, L. Colomb, P. R. Gellert, M.G. Schwab and K. Kim, *Nature*, 2012,**490**, 192.
- 14 P. Laaksonen, M. Kainlauri, T. Laaksonen, A. Shchepetov, H. Jiang, J. Ahopelto and M. B. Linder, *Angew. Chem. Int. Ed.*, 2010, **49**, 4946.
- 10 15 Y. Ohno, K. Maehashi and K. Matsumoto, *J. Am. Chem. Soc.*, 2010, **132**, 18012.
- 16 H. F. Zhang, Y. J. Han, Y. J. Guo and C. Dong, *J. Mater. Chem.*, 2012, **22**, 23900.
- 17 J. Q. Liu, J. G. Tang and J. J. Gooding, *J. Mater. Chem.*, 2012, **22**, 12435
- 15 18 S. Alwarappan, S. Boyapalle, A. Kumar, C. Z. Li, and S. Mohapatra, *J. Phys. Chem. C*, 2012, **116**, 6556.
- 19 E. Färm, S. Lindroos, M. Ritala and M. Leskelä, *Chem. Mater.*, 2012, **24**, 275.
- 20 20 X. Meng, Y. Zhong, Y. Sun, M. N. Banis, R. Li and X. Sun, *Carbon*, 2011, **49**, 1133.
- 21 J. A. Lewis and S. M. Cohen, *Inorg. Chem.*, 2004, **43**, 6534.
- 22 B. M. Bridgewater and G. Parkin, *J. Am. Chem. Soc.*, 2000, **122**, 7140.
- 25 23 M. A. El Mhammedi and M. Achak, *J. Hazard. Mater.*, 2009, **161**,55.
- 24 C. Gao, X. Y. Yu, R. X. Xu, J. H. Liu and X. J. Huang, *ACS Appl. Mater. Interfaces*, 2012, **4**, 4672.
- 25 J. A. Rodrigues, C. M. Rodrigues, P. J. Almeida, I. M. Valente, L. M. Goncalves, R. G. Compton and A. A. Barros, *Anal. Chim. Acta*, 2011,**701**, 152
- 30 26 M. S. A. Shah, A. R. Park, K. Zhang, J. H. Park and P. J. Yoo, *ACS Appl. Mater. Interfaces*, 2012, **4**, 3893.
- 27 X. Sun, M. Xie, G. K. Wang, H. T. Sun, A. S. Cavanagh, J. J. Travis, S. M. George and J. Lian, *J. Electrochem. Soc.*, 2012, **159**, A364.
- 35 28 P. Y. Dong, Y. H. Wang, L. N. Guo, B. Liu, S. Y. Xin, J. Zhang, Y. R. Shi, W. Zeng and S. Yin, *Nanoscale*, 2012, **4**, 4641.
- 29 T. W. Lu, R. B. Zhang, C.Y. Hu, F. Chen, S.W. Duo and Q. H. Hu, *Phys. Chem. Chem. Phys.*, 2013, **15**, 12963.
- 40 30 W. Hummers and R. J. Offeman, *J. Am. Chem. Soc.*, 1958, **80**, 1339.
- 31 X. B. Meng, D. S. Geng, J. Liu, R. Y. Li and X. L. Sun, *Nanotechnology*, 2011, **22**, 165602.
- 45 32 X. Sun, M. Xie, J. J. Travis, G. K. Wang, H. T. Sun, J. Lian, and S. M. George, *J. Phys. Chem. C*, 2013, **117**, 22497.
- 33 C. M. Ban, M. Xie, X. Sun, J. J. Travis, G. K. Wang, H. T. Sun, A. C. Dillon, J. Lian and S. M. George, *Nanotechnology*, 2013, **24**, 424002.
- 50 34 A. V. Murugan, T. Muraliganth and A. Manthiram, *Chem. Mater.*, 2009, **21**, 5004.
- 35 S. Sakthive and H. Kisch, *Angew. Chem., Int. Ed.* 2003, **42**, 4908.
- 36 H. Zhang, X. J. Lv, Y. M. Li, Y. Wang and J. H. Li, *ACS Nano*, 2010,**4**,380.
- 55 37 S. Park, J. H. An, R. D. Piner, I. Jung, D. X. Yang, A. Velamakanni, S. T. Nguyen and R. S. Ruoff, *Chem. Mater.*,2008, **20**, 6592.
- 38 Y. Wen, H. Ding and Y. Shan, *Nanoscale*, 2011, **3**, 4411.
- 39 B. S. Huang, H. H. Tseng, and M. Y. Wey, *J. Ceram. Soc. Jpn.*, 2009, **117**, 753.
- 60 40 X. B. Yan, B. K. Tay, and Y. Yang, *J. Phys. Chem. B*, 2006, **110**, 25844.
- 41 G. M. An, W. H. Ma, Z. Y. Sun, Z. M. Liu, B. X. Han, S. D. Miao, Z. J. Miao, and K. L. Ding, *Carbon*, 2007, **45**, 1795.
- 42 Q. Wang, D. Yang, D. M. Chen, Y. B. Wang, and Z. Y. Jiang, *J. Nanopart. Res.*, 2007, **9**, 1087.
- 65 43 H. F. Zhang, S. M. Shuang, L. L. Sun, A. J. Chen, Y. Qin and C. Dong, *Microchim. Acta*, 2014,**181**,189.
- 44 H. J. Chen, Y. L. Wang, Y. Liu, Y. Z. Wang, L. Qi and S. J. Dong, *Electrochem. Commun.*, 2007, **9**, 469.
- 70 45 X. Y. Yu, Q. Q. Meng, T. Luo, Y. Jia, B. Sun, Q. X. Li J. H. Liu and X. J. Huang, *Sci. Rep.*, 2013, **3**, 2886.
- 46 Y. C. Si and E. T. Samulski, *Nano Lett.*, 2008, **8**,1679.
- 47 S. Prakash and V. K. Shahi, *Anal. Methods*, 2011, **3**, 2134
- 48 M. Mališić, A. Janošević, B. Š. Paunković, I. Stojković, G. Ćirić-Marjanović, *Electrochimica Acta*, 2012,**74**, 158.
- 75 49 C. G. Hu, K. B. Wu, X. Dai and S. S. Hu, *Talanta*, 2003, **60**, 17.
- 50 L. Chen, Z. H. Su, X. H. He, Y. Liu, C. Qin, Y. P. Zhou, Z. Li, L. H. Wang, Q. J. Xie and S. Z. Yao, *Electrochem. Commun.*, 2012,**15**, 34.
- 80
- 85

- A table of contents entry.

This should include:

* Colour graphic: maximum size 8 cm x 4 cm

* Text: one sentence, of maximum 20 words, highlighting the novelty of the work.



Graphene coated with TiO₂ by atomic layer deposition exhibits markedly enhanced sensitivity for detection of heavy metal ions.